land

MDPI

Article

Spatiotemporal Assessment and Obstacle Diagnosis of Cultivated Land Quality Under Rapid Urbanization: Evidence from Chengdu, China

Huaifei Ouyang, Yisen Liu, Xinyue Peng, Yixi Zhu, Jiayan Li and Yongheng Rao *

School of Public Administration, Sichuan University, Chengdu 610065, China
* Correspondence: raoyongheng@126.com or raoyongheng@scu.edu.cn

Abstract

Conventional static approaches to cultivated land quality (CLQ) assessment often fail to capture the rapid spatial restructuring of cultivated land in urbanizing regions. This study takes Chengdu, China, as the study area and employs multi-source and multi-indicator datasets from 2010, 2017, and 2023 to assess CLQ using an integrated AHP-CRITIC weighting approach, combined with obstacle degree and constraint factor analyses. The results show that the mean CLQ score increased from 0.520 in 2010 to 0.695 in 2023, reflecting the continuous improvement in stable cultivated land quality. Constraint factors also shifted from natural endowment limitations to engineering- and management-related disturbances: converted land was mainly constrained by climatic and topographic conditions, newly added land by soil moisture and fertility after land-use conversion, and stable land by compound soil-water and terrain constraints. These findings provide scientific evidence and practical references for high-standard farmland construction and refined cultivated land governance in rapidly urbanizing grain-producing regions.

Keywords: cultivated land quality; AHP-CRITIC weighting; obstacle degree model; spatiotemporal evolution; multi-source data; Tianfu Granary

1. Introduction

Cultivated land is the material foundation of agricultural production and a strategic resource for food security. In China, the implementation of the strategy of "storing grain in land and technology" has shifted farmland protection from a focus on quantity alone toward the coordinated protection of quantity, quality, and ecology. However, cultivated land resources remain under dual pressure from continuous occupation by construction land and the deterioration of soil and ecological functions [1,2]. Globally, urban encroachment preferentially displaces crop production from fertile peri-urban soils, with the compensatory land demand substantially exceeding the area directly converted [3], and global cultivated land spatial transformation has entered a phase of net contraction since 2005, with quality differentiation intensifying across regions [4]. Sustainable intensification has emerged as a critical strategy to reconcile food security with land conservation in rapidly urbanizing regions [5], with urban-rural transition dynamics in rapidly growing metropolitan areas further confirming the vulnerability of peri-urban agricultural land to urban expansion pressures [6]. High-quality cultivated land is being lost in many rapidly urbanizing regions, while the potential for developing reserve cultivated land is increasingly limited [7]. Intensive land use, soil contamination, erosion, and fragmentation further weaken the

Academic Editors: Debin Lu, Yahui Wang, Min Cao and Yingbin Feng

Received: 28 May 2026
Revised: 26 June 2026
Accepted: 30 June 2026
Published: 5 July 2026

productive and ecological functions of farmland, making scientific and dynamic CLQ assessment a prerequisite for sustainable farmland protection [8].

CLQ evaluation has evolved from single-factor assessments of soil fertility and production potential to multidimensional frameworks that incorporate soil properties, ecological conditions, infrastructure, and land-use efficiency [9–13]. Correspondingly, evaluation methods have shifted from expert-based qualitative judgement to quantitative and integrated approaches, including entropy weighting, principal component analysis, machine learning, and combined subjective–objective weighting methods [14–17]. Multi-source remote sensing, ground monitoring, and geospatial platforms such as Google Earth Engine (GEE) have further improved the capacity to monitor farmland quality over broad areas and long time periods [18–23]. Nevertheless, two limitations remain. First, many studies still emphasize static quality grading and do not sufficiently distinguish between genuine quality improvement and compositional changes caused by the conversion, addition, or persistence of cultivated land. Second, obstacle factor diagnosis is often conducted for a single time point or at an aggregate regional scale, making it difficult to identify how constraints differ among stable, newly added, and converted cultivated land.

Chengdu, a major grain-producing region in western China and the core of the Tianfu Granary, provides a representative case for examining CLQ change under the combined influence of complex terrain, strong policy intervention, and rapid urban expansion. This study evaluates CLQ in Chengdu for three key years, 2010, 2017, and 2023, and addresses three questions: (1) How does CLQ change when cultivated land area shrinks under rapid urbanization? (2) Are observed improvements driven by real quality enhancement or by spatial replacement resulting from farmland conversion? (3) How do residual obstacle factors differ among stable, newly added, and converted cultivated land? The innovations of this paper carry global implications. Methodologically, this study constructs a closed-loop framework. The AHP-CRITIC hybrid weighting algorithm can adjust indicator systems and weight thresholds according to natural conditions and land policies of different countries and regions, overcoming the defects of single static evaluation models. This paper can provide empirical evidence for balancing urban development and farmland protection in similar grain-producing regions worldwide.

The remainder of this paper is organized as follows. Section 2 describes the study area, data sources and integrated evaluation methodology. Section 3 analyzes the spatiotemporal evolution of cultivated land quality and the differentiated obstacle factors across different farmland transition types in Chengdu. Section 4 discusses targeted improvement strategies, the international applicability of the framework, research limitations and future prospects, and summarizes the core conclusions.

2. Materials and Methods

2.1. Description of the Study Area

Chengdu, the capital of Sichuan Province, is a major grain-producing region in western China and the core area of the Tianfu Granary. Its terrain is higher in the northwest and lower in the southeast, forming a pattern commonly described as “one-third plains, one-third hills, and one-third mountains,” which creates diverse conditions for agricultural land use (Figure 1). The city has a crop-sown area of more than 10 million mu, including more than 5.7 million mu of grain crops, and therefore plays an important role in regional food security. At the same time, rapid urbanization has intensified pressure on cultivated land through construction-land expansion, conflicts between agricultural production and ecological protection, and rising demand for quality conservation and improvement [24,25]. These characteristics make Chengdu an appropriate case for developing a dynamic CLQ evaluation and obstacle diagnosis framework.

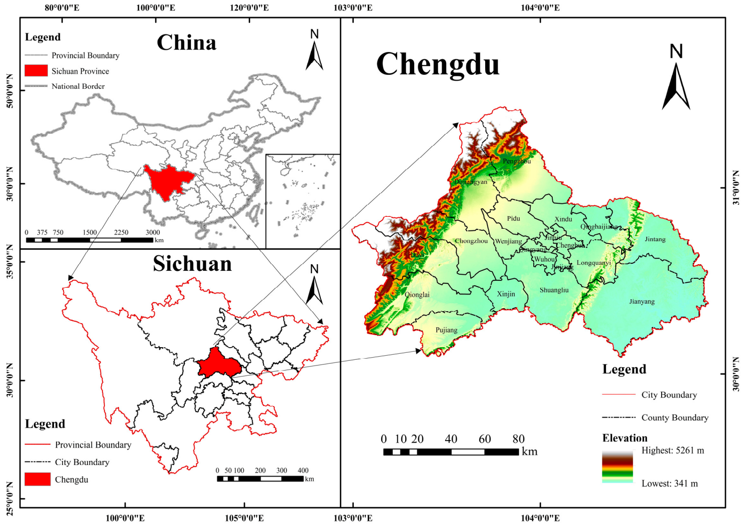

Figure 1. Geographical location and extent of Chengdu. The base map was produced using a standard map downloaded from the Standard Map Service of the Ministry of Natural Resources (approval number GS(2019)3333), and the base-map boundary was not modified.

2.2. Research Methods

2.2.1. Research Framework

This study selected 2010, 2017, and 2023 as representative policy years and used Chengdu as the empirical study area. Multi-source remote sensing, ground monitoring, and socioeconomic datasets were integrated to construct an 18-indicator CLQ evaluation system. Each indicator was standardized using fuzzy membership functions, and indicator weights were calculated with an AHP-CRITIC combined weighting method. CLQ scores were then estimated for the three study years, and the robustness of the results was examined using Pearson and Spearman correlation coefficients. The natural breaks (Jenks) method was used to classify CLQ into five grades. Finally, an obstacle degree model was applied to identify the key factors limiting CLQ improvement in stable, newly added, and converted cultivated land, thereby linking quality evolution with land-transition processes.

2.2.2. Cultivated Land Quality Evaluation

Cultivated land is a coupled natural-human system shaped by geomorphology, climate, soil conditions, infrastructure, and land use. Following the principles of comprehensiveness, dominance, data availability, and operational applicability, this study constructed the indicator system (Figure 2) with reference to the national standard "Cultivated land quality grade" (GB/T 33469-2016) [26] and related CLQ evaluation studies [27,28]. Considering the difficulty of obtaining spatially continuous field observations for all evaluation years, some indicators were represented by proxy variables that can reflect the corresponding ecological or productive conditions at the regional scale.

The indicator system contains five criterion layers. Geomorphological indicators describe topographic suitability and cultivation constraints [8]. Climatic indicators represent hydrothermal conditions that determine long-term production stability [29]. Soil indicators capture nutrient supply, soil water regulation, rooting depth, texture, compactness, and acidity-alkalinity [30,31]. Infrastructure indicators reflect irrigation accessibility, road connectivity, and farming convenience [32]. Land-use indicators measure actual production performance and cropping-structure suitability (Table 1).

Table 1. Cultivated Land Quality Evaluation Indicator System.

Target Layer	Criterion Layer	Indicator Layer	Indicator Meaning	Directionality
Cultivated Land Quality	Geomorphological Characteristic Indicators	Slope	Angle of surface inclination, affecting surface runoff and erosion extent	Negative
		Elevation	Vertical height of cultivated land above sea level; influences cultivated land quality through temperature, air pressure, and precipitation	Negative
		Aspect	Direction of slope aspect; determines distribution of light, temperature, and moisture	Positive
	Climatic Condition Indicators	$\geq$10 °C Accumulated Temperature	Total heat during the active growing season of crops; affects multiple cropping index and biomass accumulation	Positive
		Annual Precipitation	Determines regional water supply capacity; influences soil moisture balance and nutrient cycling	Positive
	Soil Condition Indicators	Soil Fertility	Comprehensively reflects the nutrient supply potential of cultivated land	Positive
		Soil Moisture	Relative state of soil wetness or dryness and water retention capacity	Moderate
		Organic Carbon Content	Reflects soil fertility and microbial activity	Positive
		Biodiversity	Reflects the structural complexity and stability of the cultivated land ecosystem	Positive
		Effective Soil Layer Thickness	Affects crop root development and water/nutrient storage capacity	Positive
		Plough Layer Texture	Soil particle composition affects aeration, water permeability, and nutrient retention capacity	Moderate
		Soil Bulk Density	Measures soil compactness; affects soil aeration and workability	Negative
		pH Value	Reflects soil acidity or alkalinity; affects nutrient availability	Moderate
	Infrastructure Condition Indicators	Distance to Irrigation	Characterizes the guarantee capacity of agricultural irrigation conditions; determines drought resistance of cultivated land	Negative
		Distance to Roads	Characterizes the connection degree with the transportation system; affects machinery operation, material transport, and field management	Negative
		Distance to Settlements	Characterizes the actual distance from cultivated land to settlements or farm households; reflects farming convenience	Negative
	Land Use Condition Indicators	Grain Yield per Unit Area	Reflects the production capacity per unit land area; influenced by both natural and anthropogenic factors	Positive
		Crop Type	Characterizes cultivated land use patterns; reflects land productivity	Positive

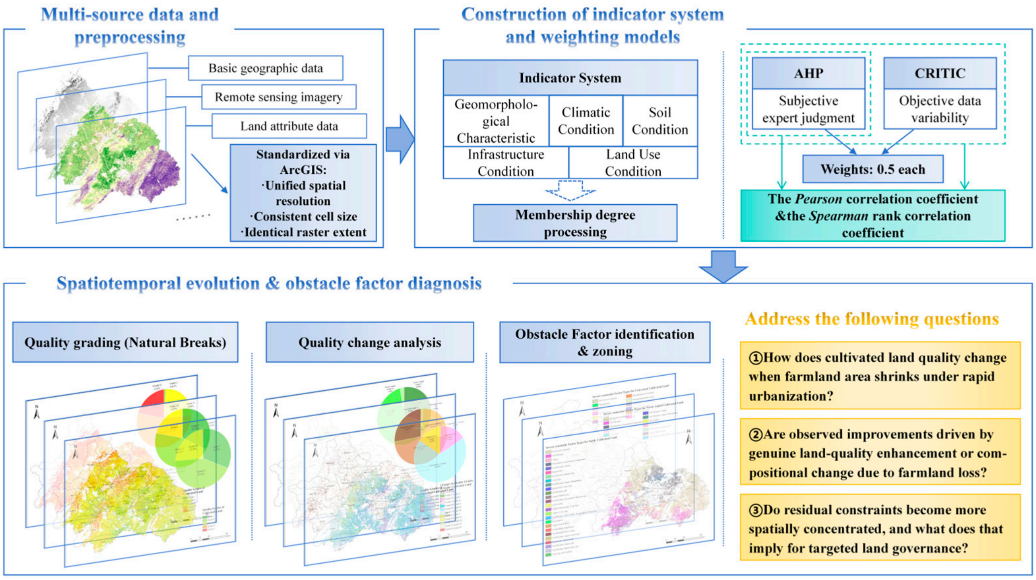

Figure 2. Technical roadmap.(Arrows and dashed box explain that Pearson & Spearman correlations are applied to compare AHP and combined AHP-CRITIC weighting results).

A subjective-objective combined weighting method was used to determine the comprehensive weight of each indicator. First, the analytic hierarchy process (AHP) was applied to obtain subjective weights [33]. Ten experts in land resource management, agroecology, and geographic information science were invited to form an evaluation panel, and the consistency ratio (CR) of all judgement matrices was controlled below 0.1. Second, the CRITIC method was used to calculate objective weights [34]. To ensure comparability across years, indicator data for 2010, 2017, and 2023 were pooled to estimate contrast intensity and inter-indicator conflict, generating global objective weights that reflected long-term variation.

The AHP and CRITIC weights were integrated using a linear combination:

$$\omega_i^{(comb)} = \alpha \cdot \omega_i^{(AHP)} + (1-\alpha) \cdot \omega_i^{(CRITIC)} \tag{1}$$

where $\omega_{\mathrm{i}}^{(comb)}$ is the combined weight of indicator i, $\omega_{\mathrm{i}}^{(AHP)}$ is the subjective weight derived from AHP, $\omega_{\mathrm{i}}^{(CRITIC)}$ is the objective weight derived from CRITIC, and α is the integration coefficient. To balance expert knowledge and data-driven information, α was set to 0.5, meaning that AHP and CRITIC each contributed 50% to the final weight.

CLQ scores were calculated by multiplying the standardized membership value of each indicator by its combined weight. The resulting scores were classified into five grades using the natural breaks (Jenks) method, as shown in Table 2. To support spatial visualization and grade composition analysis of CLQ, the natural breaks (Jenks) method was used to classify the continuously distributed CLQ scores into five grades for each study year separately (Table 2). This method identifies natural grouping structures within the data by minimizing within-grade variance and maximizing between-grade variance, making it well-suited for revealing spatial differentiation patterns of CLQ in each period. Using a single set of breakpoints for all periods ensures consistent grading standards for cross-year comparison of cultivated land quality spatial patterns and grade composition changes.

Table 2. Cultivated Land Quality Classification Table.

Grade	Level 1 (Best)	Level 2 (Better)	Level 3 (Moderate)	Level 4 (Poorer)	Level 5 (Poorest)
Score	0.716–0.849	0.666–0.716	0.588–0.666	0.506–0.588	0.344–0.506

2.2.3. Obstacle Factor Diagnosis

The obstacle degree model was used to diagnose the contribution of each indicator to the limitation of CLQ improvement [35,36]. The model includes three key variables: the factor contribution rate V_j, which is represented by the weight of indicator j; the indicator deviation degree B_j, which measures the gap between the membership degree A_j and the ideal value of 1; and the obstacle degree $\mathrm{M_j}$, which represents the relative limiting effect of indicator j on the overall CLQ level. The formulas are as follows:

$$B_j = 1 - A_j \tag{2}$$

$$\mathrm{M_j} = \frac{B_j\,V_j}{\sum_{j=1}^{n} B_j\,V_j} \times 100\% \tag{3}$$

Based on the above formulas, obstacle degrees were calculated for 2010, 2017, and 2023. Indicators with an obstacle degree of at least 5% were identified as major obstacle factors [37]. Following the equal-interval classification method, obstacle degrees were divided into severe restriction (>15%), moderate restriction (10–15%), mild restriction (0–10%), and no restriction (0%) [38].

2.2.4. Robustness Test

To test the robustness of the CLQ evaluation method, results obtained from the AHP-CRITIC combined weighting method were compared with those obtained from the AHP-only method. Pearson correlation coefficient (r) and Spearman rank correlation coefficient (ρ) were used to quantify the consistency of CLQ scores and rankings for 2010, 2017, and 2023 [28].

2.3. Data Sources and Preprocessing

2.3.1. Data Sources

Land-use data were obtained from the Wuhan University CLCD dataset, and administrative boundary data were obtained from the standard map with approval number GS(2024)0650 provided by the National Geomatics Center of China (NGCC). Slope, elevation, and aspect were derived from the ASTER GDEM V3 dataset. The $\geq$10 °C accumulated temperature and annual precipitation were obtained from the ERA5-Land dataset on GEE (Google LLC, Mountain View, CA, USA) and the China 1 km monthly precipitation dataset released by the National Tibetan Plateau Data Center, respectively. Soil fertility was characterized using NDVI calculated from Landsat 5 TM and Landsat 8 OLI/TIRS imagery on GEE. Although NDVI does not directly measure soil nutrients, it reflects vegetation vigor and can indirectly capture the integrated effects of soil nutrient supply, soil moisture, and crop growth conditions at the regional scale. Soil moisture was derived from the GLEAM4 dataset. Biodiversity was represented by the Shannon Diversity Index (SHDI) calculated from CLCD land-use data. SHDI does not directly represent species-level biodiversity, but it reflects landscape heterogeneity and habitat structural complexity around cultivated land, which are relevant to the ecological dimension of cultivated land quality. Organic carbon content, effective soil layer thickness, plough layer texture, bulk density, and pH were obtained from the Basic Soil Property Dataset of High-Resolution China Soil Information Grids. Infrastructure indicators were calculated using Euclidean distances to roads, irrigation sources, and settlements based on OSM data and the Global Urban and Rural Settlement (GURS) dataset. Grain yield per unit area was obtained from the Chengdu Statistical Yearbooks of 2011, 2018, and 2024. Crop type was represented by a weighted composite score based on expert evaluation and the China 1980–2022 annual spatial distribution dataset of 14 crop types from Tsinghua University. Because the crop-type dataset had not released 2023 data, the 2022 crop-type spatial pattern was used as a proxy for 2023 to maintain temporal continuity. This substitution introduces only slight uncertainty. A long-term comparison using the same dataset (2010–2022) confirms minimal interannual fluctuation of cropping patterns in Chengdu at the municipal scale. With low indicator weight, it does not alter overall CLQ trends or core conclusions, and minor deviations are limited to scattered small plots.

2.3.2. Primary Processing

To ensure spatial comparability among datasets, all data were clipped to the administrative boundary of Chengdu using ArcGIS 10.8 (Esri, Redlands, CA, USA) and resampled to a uniform spatial resolution of 30 m × 30 m. This processing ensured that all indicator layers were aligned with the cultivated land raster in projection, resolution, and pixel correspondence.

To remove dimensional effects and make indicators comparable, membership functions were used to standardize all indicators. For positive indicators, where larger values indicate higher CLQ, an upper-limit S-shaped function was used. For negative indicators, where larger values indicate lower CLQ, a lower-limit inverse S-shaped function was adopted. For moderate indicators with an optimal range, such as soil moisture and pH, a peak function was used. Plough layer texture was treated as a qualitative indicator and assigned membership values according to texture classes. The parameters used for numerical indicators and qualitative classes are shown in Tables 3 and 4.

Table 3. Membership Function Parameters for Numerical Indicators.

Directionality	Function Type	Indicator	a1	b1	b2	a2
Positive	Upper-limit (S-shaped) $\mu(x) = \begin{cases} 1 & x \geq a_2 \\ \frac{x-a_1}{a_2-a_1} & a_1 < x < a_2 \\ 0 & x \leq a_1 \end{cases}$	Aspect	166.828			182.476
		≥10 °C Accumulated Temperature	4294.466			6347.098
		Annual Precipitation	999.404			1559.148
		Soil Fertility	0.207			0.602
		Organic Carbon Content	8.532			12.911
		Biodiversity	0.099			0.579
		Effective Soil Layer Thickness	89.687			139.565
		Grain Yield per Unit Area	5254			6020.249
Negative	Lower-limit (inverse S-shaped) $\mu(x) = \begin{cases} 1 & x \leq a_1 \\ \frac{a_2-x}{a_2-a_1} & a_2 < x < a_1 \\ 0 & x \geq a_2 \end{cases}$	Slope	0.353			0.797
		Elevation	440.292			705.012
		Soil Bulk Density	1166.510			1299.048
		Distance to Irrigation	1.628			938.688
		Distance to Roads	0.268			2073.063
		Distance to Settlements	0.640			2514.003
Moderate	Peak (parabolic) $\mu(x) = \begin{cases} 1 & b_2 \geq x \geq b_1 \\ \frac{x-a_1}{b_1-a_1} & a_1 < x < b_1 \\ \frac{x-a_2}{b_2-a_2} & a_2 > x > b_2 \\ 0 & x \leq a_1, x \geq a_2 \end{cases}$	Soil Moisture	0.4	0.6	0.7	0.8
		pH Value	5.5	6.5	7.5	8.5

Table 4. Membership Degree for Qualitative Indicators.

Directionality	Indicator	Level 1		Level 2		Level 3		Level 4	
		Indicator Value	Score	Indicator Value	Score	Indicator Value	Score	Indicator Value	Score
Moderate	Plough Layer Texture	Loam, Silt loam	1	Sandy clay loam, Clay loam, Silty clay loam	0.7	Silt, Sandy loam	0.4	Sandy clay	0.3

3. Results

3.1. Spatial Patterns and Grade Distribution of Cultivated Land Quality

3.1.1. Spatial Pattern and Differentiation of Cultivated Land Quality

The spatial distribution of CLQ grades in Chengdu for 2010, 2017, and 2023 is shown in Figure 3. Cultivated land was largely absent from the northwestern mountainous areas and the central urban districts. Higher-quality cultivated land was concentrated in the southwestern plains and eastern shallow hills, whereas lower-quality land occurred mainly in mountain-front and hill-plain transition zones.

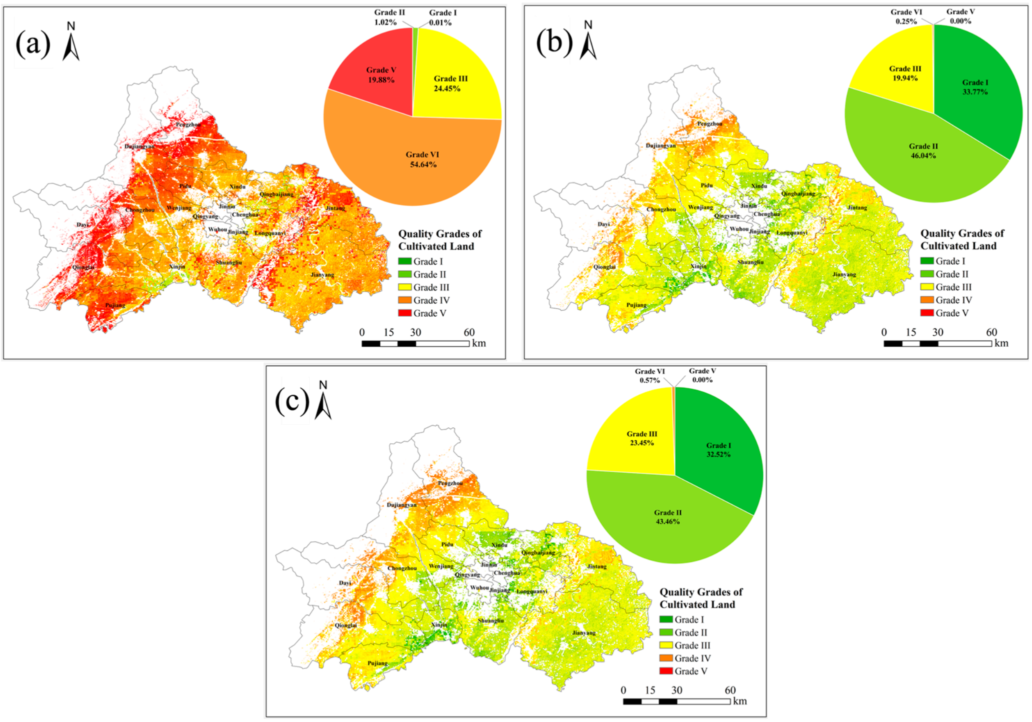

Figure 3. Spatial patterns and grade distribution of cultivated land quality in Chengdu: (**a**) 2010; (**b**) 2017; (**c**) 2023.

In 2010, the overall CLQ level was relatively low and high-quality cultivated land was highly fragmented. Grade 5 land was mainly distributed along the Longmen Mountains in western Chengdu and the Longquan Mountains in the east, while Grade 4 land was widespread in the eastern shallow hills and the transition zones between plains and mountains. By 2017, CLQ had improved markedly: Grades 1 and 2 formed more continuous distributions in the core plain area, and Grades 4 and 5 had shrunk substantially. In 2023, the spatial pattern was broadly stable, with further clustering of high-quality land and a slight expansion of Grade 3 land in peripheral shallow hilly areas.

These results indicate that the initial CLQ baseline in 2010 was constrained by weak infrastructure and fragmented land use, especially in hilly-plain transition zones. The subsequent expansion of high-standard farmland construction and comprehensive land consolidation in areas such as Xinjin District and Qionglai City substantially improved the regional CLQ baseline through land leveling, irrigation and drainage improvement, and plot consolidation.

3.1.2. Area Composition and Distribution of Cultivated Land Quality Grades

As shown in Table 5, the proportion of high-quality cultivated land increased substantially after 2010. In 2010, Grades 4 and 5 accounted for 74.52% of the total cultivated land area, whereas Grades 1 and 2 were scarce. By 2017, Grades 1 and 2 accounted for 79.80%, and Grade 5 had almost disappeared (0.01 km^2). In 2023, Grades 1 and 2 still accounted for 75.97% of the total cultivated land area, while Grades 4 and 5 remained very limited (0.57% and approximately 0%, respectively).

Table 5. Area and proportion of cultivated land quality grades in Chengdu in 2010, 2017, and 2023.

Grade	2010		2017		2023	
	Area/km^2	Percentage/%	Area/km^2	Percentage/%	Area/km^2	Percentage/%
1	0.64	0.01	2805.02	33.77	2545.08	32.52
2	89.21	1.02	3824.78	46.03	3402.41	43.46
3	2131.33	24.45	1652.99	19.94	1831.27	23.45
4	4763.00	54.64	21.05	0.25	44.59	0.57
5	1733.43	19.88	0.01	0	0.01	0
Total	8717.61	100	8303.85	100	7823.36	100

3.1.3. Robustness Test Results

The robustness test showed strong agreement between the AHP-CRITIC and AHP-only results. The Pearson correlation coefficients for 2010, 2017, and 2023 were 0.880, 0.873, and 0.888, respectively, and the Spearman rank correlation coefficients were 0.858, 0.856, and 0.877, respectively. These consistently high correlations indicate that the CLQ evaluation and grade classification were stable across weighting schemes (Figure 4).

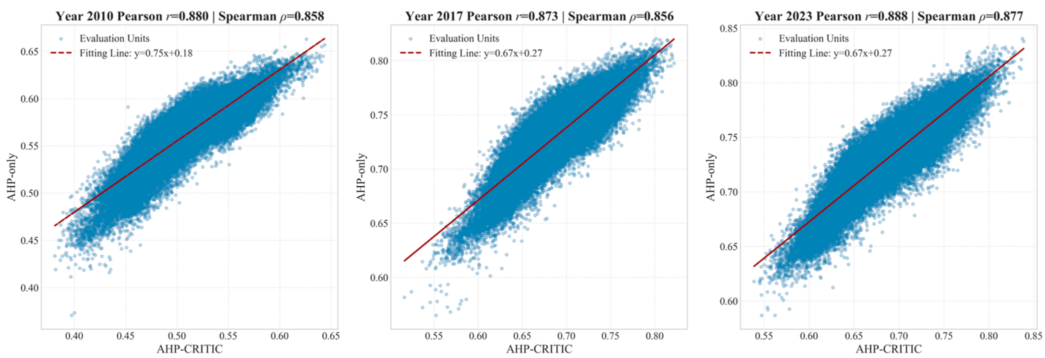

Figure 4. Robustness test results.

3.2. Spatiotemporal Dynamics of Cultivated Land Quality

3.2.1. Overall Temporal Dynamics in Cultivated Land Quality

Mean CLQ scores reveal a clear improvement followed by stabilization. The mean CLQ score increased from 0.520 in 2010 to 0.698 in 2017 and then remained nearly stable at 0.695 in 2023 (Figure 5). This pattern indicates that cultivated land protection and improvement policies generated substantial gains before 2017, whereas subsequent improvements became more limited.

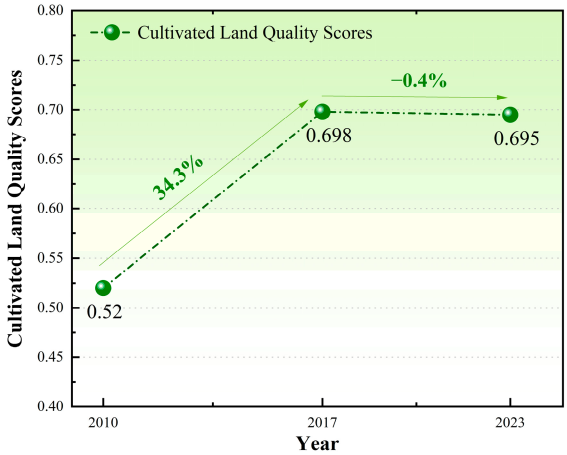

Figure 5. Changes in mean cultivated land quality scores in Chengdu, 2010–2023.

Specifically, 2010–2017 was a rapid improvement stage, during which the mean CLQ score increased by 34.3%. In contrast, 2017-2023 was a stabilization stage, with the mean score decreasing slightly by 0.4%. This marginal decline, however, should not be interpreted as a deterioration of stable cultivated land. As shown in Table 6, over 99% of stable cultivated land actually improved during 2010–2023. The slight decrease in the average score is primarily a compositional effect: some medium-quality and high-quality peri-urban farmland was converted to construction uses in rapidly urbanizing districts such as Shuangliu and Tianfu New Area, while newly added land largely obtained from land consolidation entered the cultivated land pool with an initial quality deficit that had not yet been fully remediated by 2023. This spatial replacement temporarily lowered the average score, masking the continued improvement of stable plots. Moreover, by 2017, most farmland amenable to large-scale engineering measures like land leveling, irrigation channels, and field roads had already been upgraded. The remaining constraints, such as soil organic matter restoration, biodiversity enhancement, and soil structure recovery after mechanical disturbance, are inherently slower to resolve and require ecological rather than engineering approaches. The 0.4% decline thus signals the onset of a more challenging stage requiring refined, long-term management.

Table 6. Types, areas, and proportions of cultivated land quality change.

Type of Cultivated Land Quality Change	Area (km^2)	Proportion (%)	
No change	23.29	0.26%	0.26%
Newly added Grade I	162.35	1.84%	5.93%
Newly added Grade II	162.61	1.85%	
Newly added Grade III	184.89	2.10%	
Newly added Grade IV	12.45	0.14%	
Newly added Grade V	0.01	0.00%	
Converted Grade I	0.17	0.00%	11.16%
Converted Grade II	14.20	0.16%	
Converted Grade III	250.17	2.84%	
Converted Grade IV	465.84	5.29%	
Converted Grade V	252.85	2.87%	
Upgraded by four grades	15.65	0.18%	82.64%
Upgraded by three grades	1214.01	13.79%	
Upgraded by two grades	4997.0601	56.74%	
Upgraded by one grade	1051.0209	11.93%	
Degraded by one grade	0.02	0.00%	0.00%

3.2.2. Spatial Differentiation of Cultivated Land Quality Change

From 2010 to 2023, CLQ change showed pronounced spatial differentiation (Figure 6; Table 6). Quality improvement was the dominant transition type, accounting for 82.64% of the study area, followed by converted cultivated land (11.16%) and newly added cultivated land (5.93%). Among stable cultivated land, more than 99% experienced quality improvement, mainly by two grades (68.44%), followed by three-grade and one-grade improvements (Figure 7). Degradation was almost absent. Newly added cultivated land was concentrated in Grades I–III, whereas converted cultivated land was concentrated in Grades III–V (Figure 8). This structure suggests a one-directional optimization process in which low-quality land tended to be converted, medium-quality land was upgraded, and high-quality land was supplemented.

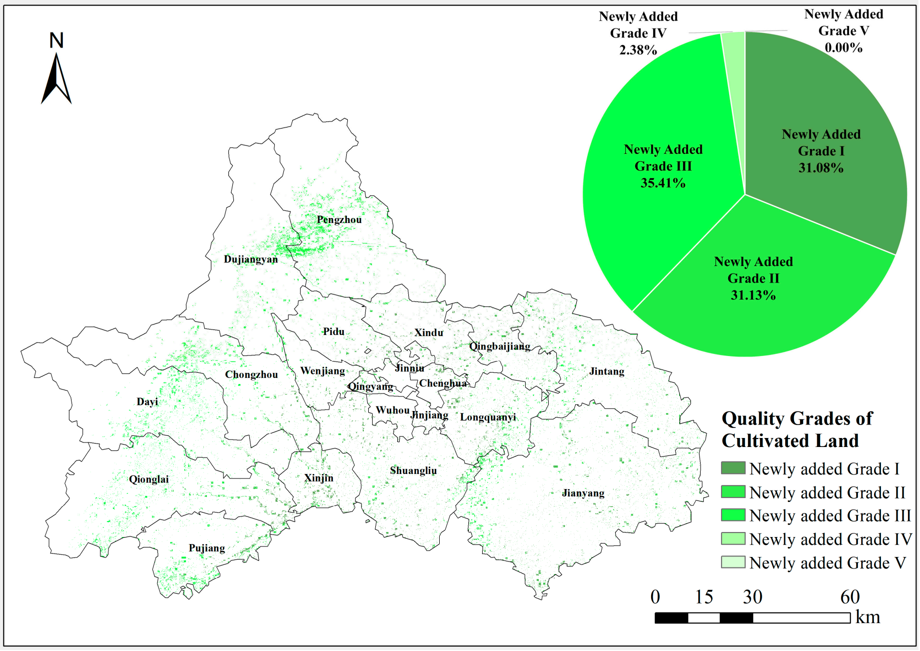

Figure 6. Quality grades of newly added cultivated land in Chengdu, 2010–2023.

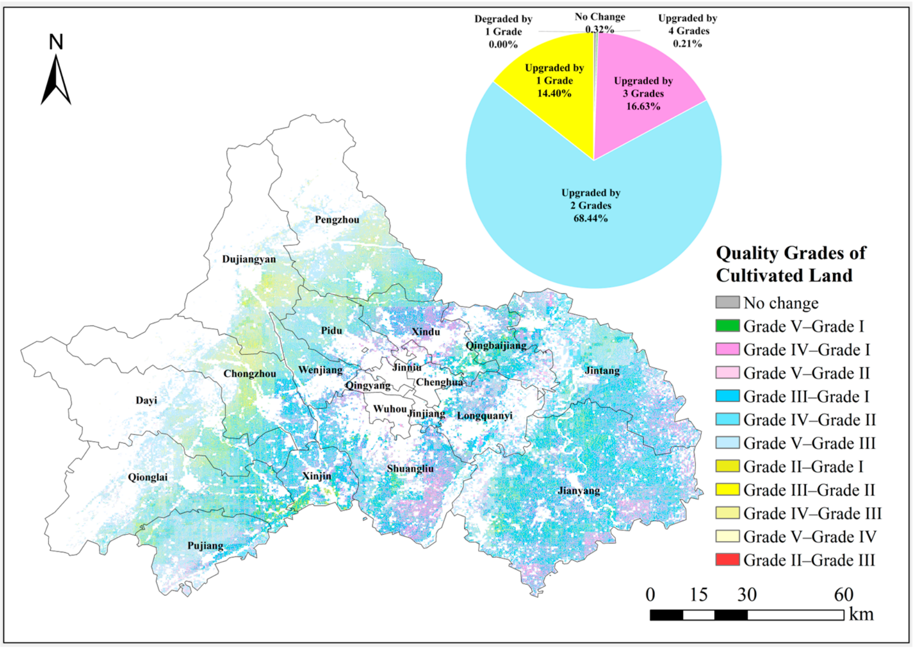

Figure 7. Quality-grade changes in stable cultivated land in Chengdu, 2010–2023.

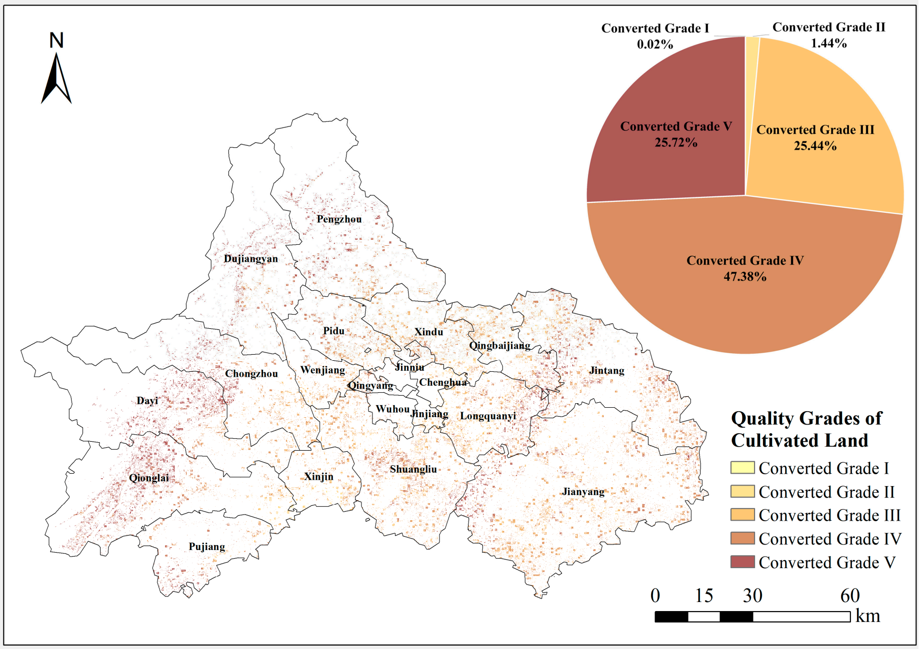

Figure 8. Quality grades of converted cultivated land in Chengdu, 2010–2023.

Spatially, CLQ change formed a concentric pattern of "stable core-peri-urban conversion-outer-suburban improvement and supplementation." Newly added cultivated land was mainly distributed in peripheral areas with relatively favorable terrain and consolidation potential. Converted cultivated land clustered in peri-urban zones affected by urban expansion. Improvements in stable cultivated land were widespread, with the largest gains occurring in outer suburban areas dominated by medium and low-grade cultivated land.

The transition pathway was hierarchical: medium-grade land was the main source of upgrading, high-grade land showed only marginal improvement, and low-grade land was more likely to exit cultivated use. This pattern reflects the combined effects of cultivated land requisition-compensation balance, high-standard farmland construction, and comprehensive land consolidation, which jointly promoted quality improvement and spatial optimization.

Regionally, differentiated improvement strategies were observed. In Chongzhou, high-quality cultivated land development was supported by the construction of a National Modern Agricultural Industrial Park, a 100,000 mu national Grade I high-quality rice production base, and the continued deepening of the agricultural co-management system [34]. In Xinjin District and Qionglai, comprehensive measures such as high-standard farmland construction, soil pollution control, requisition-compensation balance, and farmland stewardship improved fragmented cultivated land through plot merging, land leveling, and irrigation-drainage infrastructure upgrading [35].

3.3. Spatiotemporal Pattern and Zoning of Constraint Factors

The constraint factors for converted cultivated land were strongly associated with the physical geographical pattern. Precipitation-dominated constraints were concentrated in the central-eastern part of the study area, where mountain interception reduces effective precipitation and increases dependence on irrigation. Aspect-dominated and aspect-precipitation compound constraints mainly appeared in the western mountain-plain transition zone, where shaded slopes and terrain relief limit solar radiation, heat accumulation, and mechanized farming. Soil moisture constraints were also concentrated in parts of the southwest, where insufficient water-conservancy support and weak soil water-regulation capacity reduced the long-term viability of cultivation. These patterns indicate that converted cultivated land was often located in areas with relatively unfavorable natural conditions and higher maintenance costs (Figure 9).

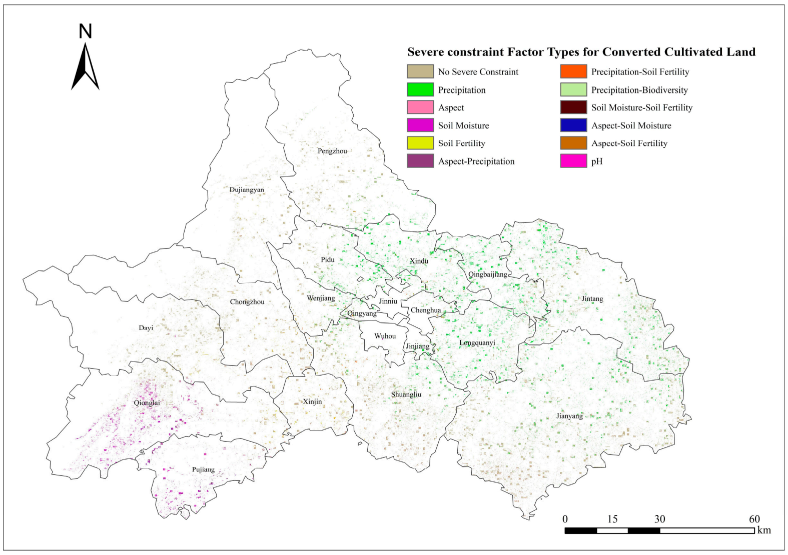

Figure 9. Zoning of severe constraint factor types for converted cultivated land.

For newly added cultivated land, the spatial pattern of constraints reflected the effects of land-use conversion more directly. Soil moisture-dominated constraints were concentrated in the southwestern edge of the Chengdu Plain, where former garden and forest land was converted into cultivated land. Vegetation removal, deep ploughing, and mechanical reconstruction can damage soil aggregates, reduce organic matter, and weaken soil water regulation, thereby creating short-term moisture imbalance and waterlogging risk. Non-severe constraints in the northernmost area suggest better source conditions and lower disturbance during conversion. Local precipitation-accumulated temperature compound constraints in northern and central-eastern areas indicate that some newly added cultivated land inherited natural climatic limitations, suggesting that future land supplementation should more strictly consider suitability and long-term sustainability (Figure 10).

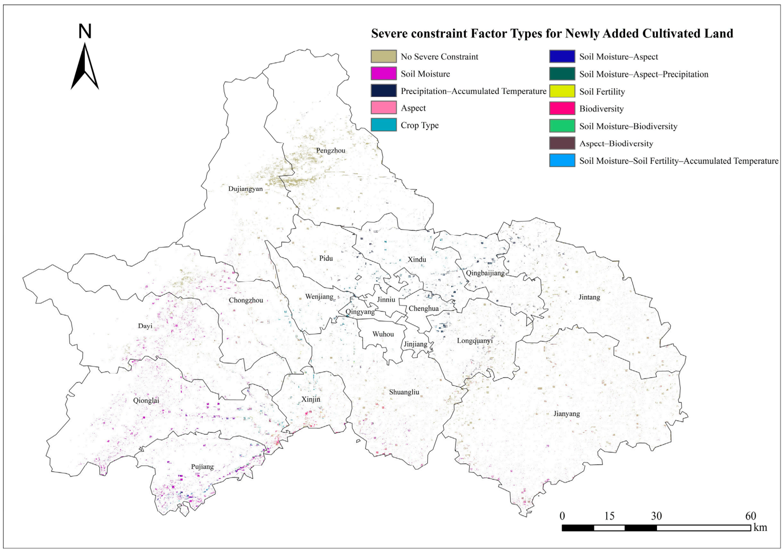

Figure 10. Zoning of severe constraint factor types for newly added cultivated land.

A comparison of converted and newly added cultivated land shows that identical constraint types may arise from different mechanisms. For example, soil moisture constraints occur in both land-transition types in the southwest, but in converted land, they mainly reflect long-term irrigation and water-regulation deficiencies, whereas in newly added land, they are more closely linked to soil structural disturbance during conversion. Therefore, obstacle diagnosis should be interpreted together with land-use history rather than by indicator type alone.

Stable cultivated land displayed the most diverse constraint structure and a clear gradient from the core Chengdu Plain to the western and northwestern mountain-front areas (Figure 11). This pattern is closely related to spatial differences in terrain, elevation, hydrothermal conditions, and soil properties. The non-severe constraint type was mainly concentrated in the core plain, where flat terrain, favorable hydrothermal conditions, and dense irrigation networks support long-term stable cultivation.

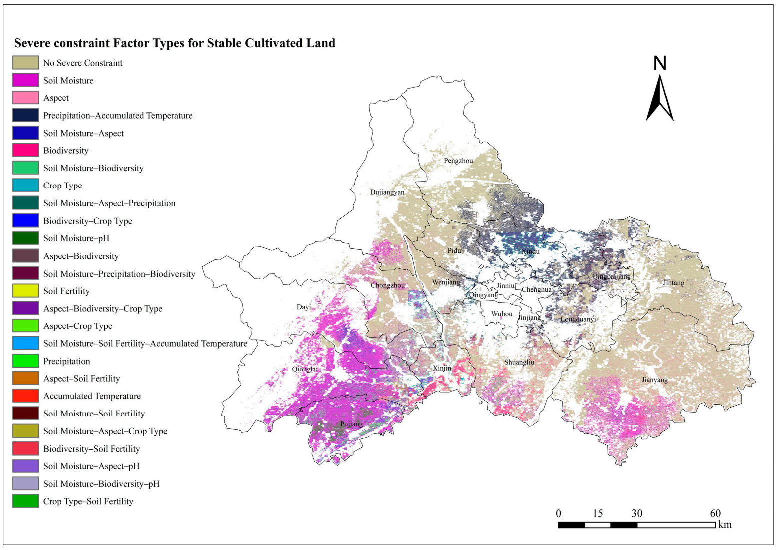

Figure 11. Zoning of severe constraint factor types for stable cultivated land.

Soil moisture-dominated constraints were widely distributed in the southwest and were associated with heterogeneous parent materials and hydrological conditions; however, these constraints remain relatively amenable to improvement through irrigation-drainage construction and soil water-regulation measures. Precipitation-accumulated temperature compound constraints were concentrated in the northern areas affected by the Longmen Mountains and represent relatively low-intervention natural limitations. Aspect-related constraints occurred mainly in the western piedmont transition zone, where slope aspect interacts with soil moisture and terrain. Biodiversity-dominated constraints were scattered across the study area, suggesting stronger links with habitat fragmentation, farming intensity, and land-use structure rather than a single physical geographical factor.

4. Discussion and Conclusions

4.1. Main Findings and Policy Implications

Based on the "evaluation-diagnosis-optimization" framework, this study assessed the spatiotemporal evolution of CLQ in Chengdu from 2010 to 2023 and interpreted the results through the transition trajectories of converted, newly added, and stable cultivated land. The main findings are as follows:

(1) CLQ in Chengdu increased substantially from 0.520 to 0.695 and reached a medium-to-high level by 2023. This improvement was not solely the result of in situ natural

evolution. Rather, it reflected the combined effects of low-quality land conversion, the supplementation of relatively high-quality cultivated land, and the cross-grade improvement in stable cultivated land. Spatial replacement therefore partly offset the pressure of urban expansion on high-quality farmland.

(2) The dominant obstacle factors shifted from natural endowment constraints toward engineering and management-related disturbances. Converted cultivated land was mainly constrained by climatic and topographic factors, newly added cultivated land by soil moisture and fertility after mechanical reconstruction, and stable cultivated land by compound soil–water and terrain constraints.

(3) Future CLQ improvement is approaching the marginal limits of conventional engineering measures such as land leveling and plot consolidation. Further improvement should focus on ecological maturation, soil structure restoration, organic matter enhancement, irrigation-drainage optimization, and long-term fertility management. The stabilization and marginal decline observed between 2017 and 2023 reinforces this conclusion: the extensive margin of engineering-driven improvement has been largely exhausted, and the next phase of quality enhancement must shift from hard infrastructure investments to soft ecological management. This transition is particularly critical for newly added cultivated land, which requires sustained management for soil structure recovery, and for stable farmland facing compound soil-water-terrain constraints that cannot be resolved by engineering alone.

From a socio-economic perspective, the differentiated obstacle patterns can be partly explained by variations in farmer management practices, land tenure stability, and cropping intensity. For peri-urban converted cultivated land, unstable land conversion expectations may reduce farmers' willingness to invest in long-term soil improvement and irrigation maintenance, which amplifies inherent topo-climatic constraints and accelerates the exit of low-quality plots. For newly added cultivated land from land consolidation, mechanical reconstruction disturbs soil structure in the short term; meanwhile, farmers' unfamiliarity with new plots and generally low-input management often make soil moisture and fertility the dominant limitations. For stable cultivated land with clear tenure, long-term high multiple-cropping intensity and relatively homogeneous planting patterns may gradually degrade soil structure and reduce farmland biodiversity, contributing to the formation of compound soil-water-terrain constraints.

These findings imply that farmland protection in rapidly urbanizing grain-producing regions should shift from uniform engineering-oriented improvement to plot-specific and process-oriented governance. In the Tianfu Granary, high-standard farmland construction should be integrated with ecological restoration, soil water-fertility regulation, and post-conversion monitoring so that quality improvement can be sustained after land consolidation projects are completed.

These dynamics are consistent with patterns identified in the broader international literature. Globally, urban encroachment preferentially displaces crop production from high-quality peri-urban soils, with similar conversion pressures documented in other rapidly urbanizing metropolitan regions in Asia, and global cultivated land transformation has entered a phase of net contraction since 2005 with quality differentiation intensifying across regions [4–7]. These parallels suggest that the evaluation-diagnosis-optimization framework developed here has relevance beyond the Chinese context, and that the shift from engineering-driven to ecologically oriented quality management observed in Chengdu may represent a generalizable transition pathway for grain-producing regions worldwide.

https://doi.org/10.3390/land15071203

4.2. Cultivated Land Quality Evolution Under Urban Development Stages

The three-period assessment shows that CLQ evolution in Chengdu was closely coupled with urban development stages and policy intervention intensity. Changes in spatial pattern, land-transition structure, and obstacle factors were not independent processes; rather, they jointly reflected the interaction between urban expansion, farmland protection policies, and the natural suitability of cultivated land (Figure 12).

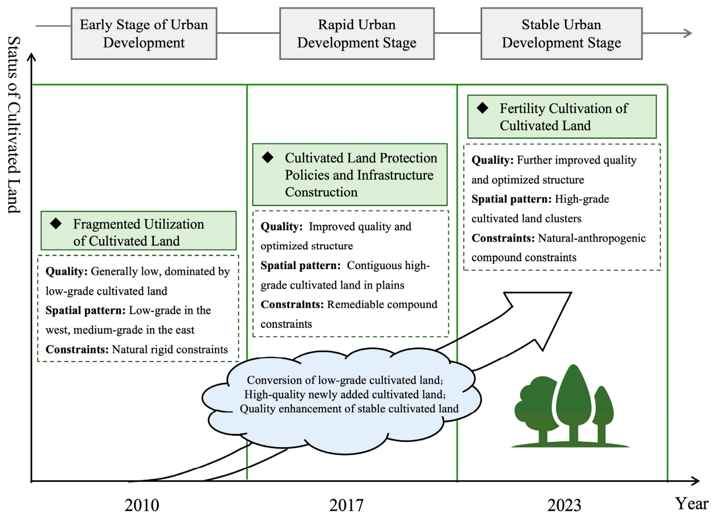

Figure 12. Evolutionary pattern of cultivated land quality driven by urban development stages. The upward arrow indicates the evolutionary trend of cultivated land quality.

In 2010, Chengdu was still in an earlier stage of rapid urban development, and policy interventions for cultivated land protection were comparatively weak. CLQ was mainly constrained by natural attributes such as precipitation and aspect, resulting in a low overall quality level and a limited amount of high-quality cultivated land.

During 2010–2017, urban development accelerated, economic capacity and infrastructure improved, and farmland protection policies were strengthened. High-standard farmland construction, comprehensive land consolidation, strict requisition–compensation balance, and the orderly withdrawal of inefficient peri-urban cultivated land jointly promoted a leap in CLQ. However, soil moisture and soil fertility constraints could not be fully resolved by short-term engineering inputs and therefore remained important limiting factors.

During 2017–2023, Chengdu entered a more stable stage of urban development, and the effects of traditional engineering transformation gradually weakened. CLQ entered a high-level stabilization stage with slight fluctuations. Newly added cultivated land showed constraints related to soil structural disturbance caused by land-use conversion, whereas stable cultivated land was increasingly characterized by compound constraints. This stage requires a stronger emphasis on endogenous soil fertility management and ecological restoration.

4.3. Advantages and Limitations of Multi-Source Data Coupling

The multi-source data framework used in this study integrates remote sensing, DEM, soil, climate, land-use, infrastructure, and statistical data, providing more comprehensive information than any single dataset. This integration supports high-resolution monitoring of CLQ dynamics and allows cultivated land to be evaluated from ecological, productive, and management-related dimensions.

The indicator system was developed with reference to GB/T 33469-2016 and adjusted to the regional characteristics of Southwest China. By combining 18 indicators with AHP-

CRITIC weighting, natural breaks classification, land-transition analysis, and obstacle diagnosis, the framework captures not only where CLQ improved or declined but also why different land-transition types face distinct constraints. For the classification step, all multi-temporal CLQ scores were pooled to generate one set of fixed Jenks breakpoints, which guarantees consistent grade boundaries for cross-year comparison. Even though unified natural breakpoints support intertemporal comparison, future research pursuing more rigid, universal grading standards may adopt fixed threshold or percentile-based classification schemes.

Several limitations remain. First, the datasets used in this study were obtained from different platforms, including the National Tibetan Plateau Data Center, GEE, soil-grid products, OSM, and Chengdu Statistical Yearbooks. Differences in acquisition standards, spatial resolution, temporal frequency, and data accuracy may introduce uncertainty during resampling, spatial allocation, and indicator standardization.

Second, the transferability of the framework depends on local data availability, regional environmental conditions, and management practices. Southwest China is characterized by complex topography and fragmented land use; therefore, when applying this approach to regions with different geographical or socioeconomic contexts, the indicator system, thresholds, and weighting scheme should be adaptively adjusted.

Third, using 2022 crop data as a proxy for 2023 creates minor micro-scale uncertainty. Future work will adopt official 2023 crop datasets to improve accuracy.

Fourth, the independent validation of CLQ results remains limited. Although actual crop yield, official cultivated land quality grades, and field survey data would be useful for validation, their use is constrained by data availability, scale mismatch, and temporal inconsistency. Grain yield per unit area has already been included in the evaluation system, so using similar yield data again may lead to circular validation. In addition, available yield statistics are generally reported at the county or district scale, whereas the CLQ results were generated at a finer spatial scale. Official quality grades and field survey data are also often unavailable, not publicly accessible, or inconsistent with the 2010, 2017, and 2023 evaluation periods. Moreover, crop yield is influenced by crop varieties, agricultural inputs, management practices, climate anomalies, and policy factors, and therefore cannot be regarded as a direct validation standard for CLQ results.

Building on these limitations, several promising directions for future research emerge.

(1) Integrating socio-economic micro-data with spatial CLQ assessment would allow a deeper understanding of the driving mechanisms behind obstacle factor differentiation. Household surveys, land tenure records, and farm management data could be linked to our grid-based CLQ results to examine how factors such as land rental duration, cropping intensity, fertilizer input, and farmers' age and education affect soil quality trajectories. This would be particularly valuable for explaining why similar natural conditions produce different constraint patterns under different management regimes. Furthermore, future studies could incorporate formal spatial autocorrelation analysis, such as Moran's I, and spatial econometric modelling, such as Geographically Weighted Regression, to strengthen the causal interpretation of CLQ driving mechanisms and spatial dependence structures identified in this study.

(2) Establishing long-term plot-level observations would validate and refine the CLQ assessment results. Fixed monitoring sites across different land transition types, such as stable, newly added, and converted would provide ground-truth data on soil physical, chemical, and biological properties over time. This would improve the calibration of membership function thresholds, validate the ecological maturation process of newly added cultivated land, and quantify the actual soil water-fertility coupling mechanisms inferred from our spatial analysis.

(3) Enhancing the transferability of our evaluation framework to other regions warrants further investigation. While the AHP-CRITIC combined weighting approach and the land-transition-based obstacle diagnosis are methodologically generalizable, the specific indicator system, membership function parameters, and weighting schemes should be adaptively adjusted to local conditions.
(4) Leveraging emerging technologies offers new opportunities for CLQ monitoring and early warning. UAV-based hyperspectral imaging could provide high-resolution soil property mapping at the field scale; IoT-based in situ sensors could enable real-time monitoring of soil moisture, temperature, and nutrient dynamics; AI-driven crop growth models could simulate future quality trajectories under different management and climate scenarios. Integrating these technologies with the evaluation framework developed in this study could support a next-generation precision farmland management system.
(5) Independent validation of CLQ results should be further strengthened. Although actual crop yield, official cultivated land quality grades, and field survey data are valuable for validation, their use in this study was constrained by data availability, scale mismatch, and temporal inconsistency. Future studies should develop independent validation datasets with consistent spatial and temporal coverage, such as plot-level yield records, official cultivated land quality grades, and field survey data, to further improve the robustness of the CLQ evaluation framework.

In addition, climate change presents an emerging challenge for CLQ sustainability. Future research should incorporate climate projections into CLQ assessments to evaluate how shifts in temperature, precipitation, and extreme weather events may affect soil properties, crop productivity, and the effectiveness of current protection measures. This is particularly important for regions like Chengdu, where the interaction between mountainous terrain and changing precipitation patterns may intensify soil erosion and water stress. Overall, this study constructs a cultivated land quality evaluation framework based on the AHP-CRITIC combined weighting method and expands the analysis perspective by distinguishing different land transition types. The findings not only present the spatial heterogeneity of cultivated land quality in the study area, but they also clarify the differentiated constraint characteristics of cultivated land with different conversion attributes, providing empirical reference for refined cultivated land management in rapidly urbanizing regions.

On the basis of addressing the above data limitations, future research can further explore the micro socio-economic driving mechanism of obstacle factor differentiation combined with farmer household surveys, and carry out long-term dynamic monitoring of cultivated land quality evolution, so as to build a more precise multi-scale cultivated land quality governance framework.

Author Contributions: Conceptualization, Y.R. and H.O.; methodology, Y.L. and H.O.; software, H.O.; validation, H.O.; formal analysis, Y.Z., X.P., J.L., Y.L. and H.O.; investigation, H.O., X.P. and Y.L.; resources, Y.R.; data curation, H.O., X.P. and Y.L.; writing—original draft preparation, Y.Z., X.P., J.L., Y.L. and H.O.; writing—review and editing, Y.R. and H.O.; visualization, H.O., Y.L., X.P., Y.Z. and Y.R.; supervision, Y.R. and H.O.; project administration, Y.R. and H.O.; funding acquisition, Y.R. All authors have read and agreed to the published version of the manuscript.

Funding: This research was funded by the National Natural Science Foundation of China (grant number 42101268).

Data Availability Statement: The data used in this study are publicly available from multiple open-access sources. The land-use data (CLCD) are available at https://doi.org/10.5194/essd-13-3907-2021 (accessed on 29 June 2026). Administrative boundary data (standard map GS(2024)0650)

are available from the National Geomatics Center of China at https://www.ngcc.cn (accessed on 29 June 2026). The ASTER GDEM V3 dataset used for slope, elevation, and aspect is available at https://doi.org/10.5067/ASTER/ASTGTM.003 (accessed on 29 June 2026). The ERA5-Land dataset used for accumulated temperature (≥10 °C) is available from the Copernicus Climate Data Store at https://doi.org/10.24381/cds.e2161bac (accessed on 29 June 2026). Monthly precipitation data are available at https://doi.org/10.5281/zenodo.3114194 (accessed on 29 June 2026). Landsat 5 TM Level-2 data and Landsat 8 OLI/TIRS Level-2 data used for NDVI calculation are available at https://doi.org/10.5066/P9IAXOVV (accessed on 29 June 2026) and https://doi.org/10.5066/P9OGBGM6 (accessed on 29 June 2026), respectively. The GLEAM4 soil moisture dataset is available at https://doi.org/10.1038/s41597-025-04610-y (accessed on 29 June 2026). The Basic Soil Property Dataset of High-Resolution China Soil Information Grids is available at https://doi.org/10.11666/00073.ver1.db (accessed on 29 June 2026). OSM road and water-network data are available at https://www.openstreetmap.org (accessed on 29 June 2026). The Global Urban and Rural Settlement Dataset (GURS) is available at https://zenodo.org/records/11160893 (accessed on 29 June 2026). The annual spatial distribution dataset of 14 crop types in China is available at https://doi.org/10.6084/m9.figshare.26028769 (accessed on 29 June 2026). The Chengdu Statistical Yearbooks (2011, 2018, and 2024) are available from the Chengdu Municipal Bureau of Statistics at https://cdstats.chengdu.gov.cn (accessed on 29 June 2026). The processed datasets generated during this study are available from the corresponding author upon reasonable request.

Acknowledgments: The authors acknowledge the data support provided by the ERA5-Land dataset, the National Tibetan Plateau Data Center, OpenStreetMap contributors, the ASTER GDEM product of METI and NASA, Landsat data provided by the U.S. Geological Survey, and the developers and contributors of the CLCD, GLEAM4, GURS, and other open-access datasets cited in the Data Availability Statement. The authors have reviewed and edited the manuscript and take full responsibility for its content.

Conflicts of Interest: The authors declare no conflicts of interest.

References

1. Foley, J.A.; DeFries, R.; Asner, G.P.; Barford, C.; Bonan, G.; Carpenter, S.R.; Chapin, F.S.; Coe, M.T.; Daily, G.C.; Gibbs, H.K.; et al. Global Consequences of Land Use. *Science* **2005**, *309*, 570–574. [CrossRef]
2. Song, W.; Pijanowski, B.C. The effects of China's cultivated land balance program on potential land productivity at a national scale. *Appl. Geogr.* **2014**, *46*, 158–170. [CrossRef]
3. Barthel, S.; Isendahl, C.; Vis, B.N.; Drescher, A.; Evans, D.L.; van Timmeren, A. Global Urbanization and Food Production in Direct Competition for Land: Leverage Places to Mitigate Impacts on SDG2 and on the Earth System. *Anthr. Rev.* **2019**, *6*, 71–97. [CrossRef]
4. Li, H.; Song, W. Spatial Transformation of Changes in Global Cultivated Land. *Sci. Total Environ.* **2023**, *859*, 160194. [CrossRef] [PubMed]
5. Kamau, H.; Roman, S.; Biber-Freudenberger, L. Nearly Half of the World Is Suitable for Diversified Farming for Sustainable Intensification. *Commun. Earth Environ.* **2023**, *4*, 446. [CrossRef]
6. Mulya, S.P.; Hudalah, D.; Prilandita, N.; Sakti, A.D. Spatio-Temporal Changes in Agricultural Land and Rural–Urban Transitions in Greater Jakarta, Indonesia. *Reg. Environ. Change* **2024**, *24*, 145. [CrossRef]
7. Kong, X. China Must Protect High-Quality Arable Land. *Nature* **2014**, *506*, 7. [CrossRef] [PubMed]
8. Duan, D.; Li, X.; Liu, Y.; Meng, Q.; Li, C.; Lin, G.; Guo, L.; Guo, P.; Tang, T.; Su, H.; et al. County-Level Cultivated Land Quality Evaluation Using Multi-Temporal Remote Sensing and Machine Learning Models: From the Perspective of National Standard. *Remote Sens.* **2024**, *16*, 3427. [CrossRef]
9. Wang, M.; Liu, X.; Liu, Z.; Wang, F.; Li, X.; Hou, G.; Zhao, S. Evaluation and Driving Force Analysis of Cultivated Land Quality in Black Soil Region of Northeast China. *Chin. Geogr. Sci.* **2023**, *33*, 601–615. [CrossRef]
10. Zornoza, R.; Acosta, J.A.; Bastida, E.; Dominguez, S.G.; Toledo, D.M.; Faz, A. Identification of Sensitive Indicators to Assess the Interrelationship between Soil Quality, Management Practices and Human Health. *Soil* **2015**, *1*, 173–185. [CrossRef]
11. Tan, Y.; Chen, H.; Lian, K.; Yu, Z. Comprehensive Evaluation of Cultivated Land Quality at County Scale: A Case Study of Shengzhou, Zhejiang Province, China. *Int. J. Environ. Res. Public Health* **2020**, *17*, 1169. [CrossRef] [PubMed]

12. Zhao, C.; Zhou, Y.; Jiang, J.; Xiao, P.; Wu, H. Spatial Characteristics of Cultivated Land Quality Accounting for Ecological Environmental Condition: A Case Study in Hilly Area of Northern Hubei Province, China. *Sci. Total Environ.* **2021**, *774*, 145765. [CrossRef]
13. Kruska, R.L.; Reid, R.S.; Thornton, P.K.; Henninger, N.; Kristjanson, P.M. Mapping Livestock-Oriented Agricultural Production Systems for the Developing World. *Agric. Syst.* **2003**, *77*, 39–63. [CrossRef]
14. Li, L.; Fu, M.; Zhu, Y.; Kang, H.; Wen, H. The Current Situation and Trend of Land Ecological Security Evaluation from the Perspective of Global Change. *Ecol. Indic.* **2024**, *167*, 112608. [CrossRef]
15. Zhang, R.; Wang, C.; Xiong, Y. Ecological Security Assessment of China Based on the Pressure-State-Response Framework. *Ecol. Indic.* **2023**, *154*, 110647. [CrossRef]
16. Jiao, M.; Wang, Y.; Hu, M.; Xia, B. Spatial Deconstruction and Differentiation Analysis of Early Warning for Ecological Security in the Pearl River Delta, China. *Sust. Cities Soc.* **2021**, *64*, 102557. [CrossRef]
17. Bastida, F.; Zsolnay, A.; Hernandez, T.; Garcia, C. Past, Present and Future of Soil Quality Indices: A Biological Perspective. *Geoderma* **2008**, *147*, 159–171. [CrossRef]
18. Xing, Y.; Liu, X.; Wang, X. Integrating UAVs, Satellite Remote Sensing, and Machine Learning in Precision Agriculture: Pathways to Sustainable Food Production, Resource Efficiency, and Scalable Innovation. *Front. Agron.* **2026**, *7*, 1670380. [CrossRef]
19. Wang, L.; Liu, S.; Song, W.; Ding, S.; Zhang, J. Global High-Resolution Forest Disturbance Type Dataset. *Earth Syst. Sci. Data* **2026**, *18*, 1601–1617. [CrossRef]
20. Liu, S.; Zhang, J.; Wang, L.; Ciais, P.; Zhang, J.; Penuelas, J.; Nath, B.; Jacquet, I.; Wu, X.; Ding, S.; et al. Mapping Previously Undetected Trees Reveals Overlooked Changes in Pan-Tropical Tree Cover. *Nat. Commun.* **2025**, *16*, 5561. [CrossRef] [PubMed]
21. Zhang, F.; Wang, G.; Hu, Y.; Chen, L.; Zhu, A.-X. Design of an Integrated Remote and Ground Sensing Monitor System for Assessing Farmland Quality. *Sensors* **2020**, *20*, 336. [CrossRef] [PubMed]
22. Li, M.; Li, H.; Zhou, Z.; Chen, Y.; Wang, Y.; Li, T.; Fu, Q. Spatial Simulation and Optimization of Cropping Structure Under Climate and Land Use Change Conditions Considering Synergistic Economic Benefits and Carbon Reduction in Crop Growth Processes. *Earth Future* **2024**, *12*, e2024EF004684. [CrossRef]
23. Heung, B.; Ho, H.C.; Zhang, J.; Knudby, A.; Bulmer, C.E.; Schmidt, M.G. An Overview and Comparison of Machine-Learning Techniques for Classification Purposes in Digital Soil Mapping. *Geoderma* **2016**, *265*, 62–77. [CrossRef]
24. Li, J.; Ding, Y.; Jing, M.; Dong, X.; Zheng, J.; Gu, L. Quantitative Change or Qualitative Change: The Impact of Whole-Region Comprehensive Land Consolidation on cultivated land Security—Based on Panel Data from Townships in Zhejiang Province. *Land* **2024**, *13*, 2158. [CrossRef]
25. Ling, L.; Tang, H.; Chen, X.; Li, S.; Han, X. Spatial Zoning and Effect Evaluation of County High-Standard Farmland Siting Delineation for Sustainable cultivated land Use in China: A Case Study in Dali, Shaanxi. *Ecol. Indic.* **2024**, *167*, 112647. [CrossRef]
26. *GB/T 33469—2016*; Cultivated Land Quality Grade. Ministry of Agriculture and Rural Affairs of the People's Republic of China: Beijing, China, 2016.
27. Lei, Y.; Guoping, C.; Junsan, Z. Layout Optimization and Division of Plateau Mountain Arable Land-Based on Cultivated Land Quality Evaluation and Local Spatial Autocorrelation. *Pol. J. Environ. Stud.* **2022**, *31*, 5083–5094. [CrossRef] [PubMed]
28. Zhuang, Q.; Wu, S.; Huang, X.; Kong, L.; Yan, Y.; Xiao, H.; Li, Y.; Cai, P. Monitoring the Impacts of Cultivated Land Quality on Crop Production Capacity in Arid Regions. *CATENA* **2022**, *214*, 106263. [CrossRef]
29. Gao, J.; Zhao, R.; Guo, Z.; Yang, Y. Transformation of cultivated land for Enhanced Quality in Northeast China: Theoretical Interpretation and Practical Evaluation. *J. Rural Stud.* **2026**, *122*, 103969. [CrossRef]
30. Yu, Z.; Kuang, L.; Jiang, Y.; Li, W.; Zhang, J.; Zhou, Y.; Guo, X.; Ye, Y. Soil Attributes Are More Important than Others in Shaping the Diversity of Cultivated Land Quality Types, Southern China. *Ecol. Indic.* **2024**, *166*, 112472. [CrossRef]
31. Liu, S.; Wang, L.; Zhang, J.; Ding, S. Opposite Effect on Soil Organic Carbon between Grain and Non-Grain Crops: Evidence from Main Grain Land, China. *Agric. Ecosyst. Environ.* **2025**, *379*, 109364. [CrossRef]
32. Li, X.; Yao, Y.; Lyu, G.; Wang, R.; Dong, X.; Zhao, Y.; Li, S.; Zhang, X.; Liu, Z. Efficient Evaluation Method for Paddy Field Quality at Plot Scale Based on Multi-Source Data and Random Forest Model. *Land Degrad. Dev.* **2025**, *37*, 2757–2777. [CrossRef]
33. Alebachew, E.D.; Dengiz, O. Multi Criteria Decision Analysis and Artificial Neural Network for Assessing Soil Quality Variation under Different Land Use and Land Cover in Samsun, Türkiye. *Environ. Sustain. Indic.* **2025**, *27*, 100737. [CrossRef]
34. Zhang, R.; Liao, Y.; Li, P.; Kong, X.; Zhao, Z.; Yao, D.; Chen, W.; Zhang, W.; Guan, M.; Dong, T. Cropland Quality Evaluation and Improvement Potential in China: Integrating Suitability, Resistance, and Contiguity. *Environ. Dev. Sustain.* **2024**, 1–29. [CrossRef]
35. Xiang, H.; Yang, Q.-Y.; Su, K.; Zhang, Z.-X. Spatiotemporal Dynamics and Obstacles of the Multi-Functionality of Land Use in Xiangxi, China. *Appl. Sci.* **2019**, *9*, 3649. [CrossRef]
36. Jing, X.; Tao, S.; Hu, H.; Sun, M.; Wang, M. Spatio-Temporal Evaluation of Ecological Security of cultivated land in China Based on DPSIR-Entropy Weight TOPSIS Model and Analysis of Obstacle Factors. *Ecol. Indic.* **2024**, *166*, 112579. [CrossRef]

37. Gong, H.; Zhao, Z.; Chang, L.; Li, G.; Li, Y.; Li, Y. Spatiotemporal Patterns in and Key Influences on Cultivated-Land Multi-Functionality in Northeast China's Black-Soil Region. *Land* **2022**, *11*, 1101. [CrossRef]
38. Wang, F.; Zhang, P.; Zhang, G.; Cui, J. Agricultural Land Quality Evaluation and Utilization Zoning Based on the Production–Ecology–Health Dimension: A Case Study of Huanghua City. *Land* **2023**, *12*, 1367. [CrossRef]